Time-Resolved Imaging and Manipulation of H_2 Fragmentation in Intense Laser Fields

Th. Ergler, A. Rudenko, B. Feuerstein, K. Zrost, C. D. Schröter, R. Moshammer, and J. Ullrich
Max-Planck-Institut für Kernphysik, D-69029 Heidelberg, Germany
(Received 27 April 2005; published 23 August 2005)

We report on the experimental realization of time-resolved coincident Coulomb explosion imaging of H_2 fragmentation in 10^{14} W/cm^2 laser fields. Combining a high-resolution "reaction microscope" and a fs pump-probe setup, we map the motion of wave packets dissociating via one- or two-photon channels, respectively, and observe a new region of enhanced ionization. The long-term interferometric stability of our system allows us to extend pump-probe experiments into the region of overlapping pulses, which offers new possibilities for the manipulation of ultrafast molecular fragmentation dynamics.

DOI: 10.1103/PhysRevLett.95.093001 PACS numbers: 33.80.Rv, 32.80.Rm, 42.50.Hz

The visualization and the possible future control of the time-dependent dynamics of quantum systems, i.e., the mapping and manipulation of a quantum mechanical wave function as it evolves in time, is one of the most fundamental challenges in contemporary atomic, molecular, and optical physics [1]. For the case of dissociating molecules, a direct method of mapping both the structure and the dynamics of nuclear wave packets was suggested by a combination of the Coulomb explosion (CE) imaging technique and a femtosecond pump-probe experiment [2–7]. As illustrated in the inset of Fig. 1, the first (pump) laser pulse prepares a molecular wave packet (e.g., initiates a dissociative ionization), and the second (probe) pulse, arriving after a certain time delay, projects the wave function onto the repulsive Coulomb potential curve. The wave packet shape is then reconstructed from the measured kinetic energy distribution of the reaction fragments using the Coulomb law. Being first applied to study the dissociation of I_2 molecules [2,3], this method was later extended to the simplest (and fastest) diatomic systems, such as H_2 [4] or D_2 [5]. The latter are the ideal candidates for testing the CE imaging schemes for two reasons. First, after the removal of both electrons they represent a pure two-center Coulomb system. Second, their fragmentation in intense laser fields was extensively studied experimentally and theoretically (see [8] and references therein).

In this Letter we report on the experimental realization of time-resolved coincident Coulomb explosion imaging of dissociating H_2 molecules. Using a combination of the "reaction microscope" spectrometer, which allows coincident detection of several charged particles with excellent momentum resolution, and a pump-probe setup providing two identical 25 fs pulses with variable delay of sub-fs accuracy, we are able to resolve in space and time the motion of two different dissociating wave packets produced by net absorption of one or two photons. We provide experimental evidences of the existence of a second maximum in the R-dependent ionization probability for H_2^+ (R denotes the internuclear distance), which was predicted in several previous theoretical studies [9–12]. Finally, we demonstrate that by using an interferometrically stable pump-probe setup which allows us to control the electric field shape in the region of overlapping pulses, a clear pump-probe experiment can be carried out even in this regime by selecting only those delays for which both pulses interfere destructively. Moreover, this simplest form of pulse shaping allows us to manipulate the ultrafast molecular fragmentation dynamics, suppressing and enhancing certain fragmentation channels.

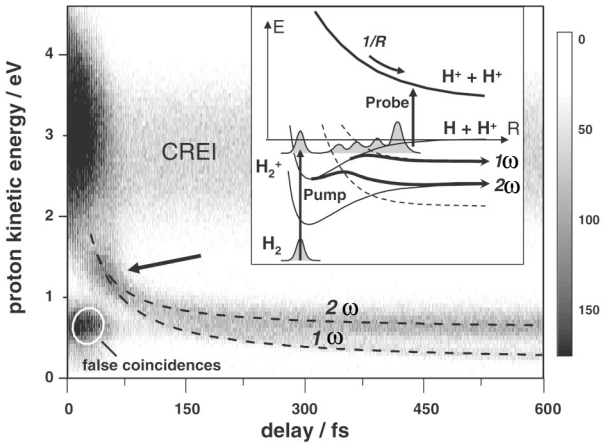

FIG. 1. The measured kinetic energy of protons created by CE of H_2 as a function of the delay between two identical 25 fs laser pulses. Plotted are only events where two protons have been detected in coincidence. Dashed lines: classically simulated wave packet propagation for dissociation of H_2^+ via 1ω and 2ω channels. The arrow indicates an enhancement corresponding to the maximum of the H_2^+ ionization rate around $R = 10$ a.u. Inset: a scheme of the pump-probe experiment. Thin lines indicate potential curves for the two lowest electronic states of H_2^+ (solid for $1s\sigma_g$, dashed for $2p\sigma_u$) dressed with n ($n = 1, 2, 3$) photons. The H_2^+ ion can dissociate either by absorbing one photon (1ω channel) or absorbing three photons in the first avoided crossing followed by a reemission of one photon at the second crossing (2ω). Since for each photon the parity of the molecular state must change, there is no direct two-photon process. For a detailed description of the dissociation mechanisms see [8,14–17,20].

The experiment was performed using linearly polarized radiation from a Kerr-lens mode locked Ti:sapphire laser at 795 nm central wavelength with 25 fs pulse width (FWHM) and 3 kHz repetition rate. The laser beam was fed through a Mach-Zehnder type interferometer with one arm variable in length, providing two identical pulses separated by a time delay which can be scanned from 0 to 1200 fs with a resolution of better than 300 as. Both laser beams were focused to a spot size of ~ 5 μm onto the collimated supersonic molecular gas jet in the center of an ultrahigh vacuum chamber (2×10^{-11} mbar). Charged reaction fragments were guided to two position-sensitive channel plate detectors by weak electric (2 V/cm) and magnetic (7 G) fields applied along the laser polarization axis. From the time-of-flight and position on the detectors the full momentum vectors of the coincident recoil ions and electrons were calculated. A detailed description of the spectrometer and the coincident measurement scheme, as well as the structure of a typical H_2 fragmentation spectrum can be found in [13,14]. Comparing the autocorrelation pattern obtained from the ion signal with the intensity autocorrelation measured with a photodiode before and after the experiment, we found very similar patterns, with only slight differences due to the higher order of nonlinearity of the ionization process. This indicates that the optical arrangement was interferometrically stable during the acquisition time of more than 50 hours.

In Fig. 1 the kinetic energy of protons created by CE of H_2 molecules is plotted as a function of the delay between the two 25 fs laser pulses. In order to separate CE events from dissociation fragments, only those events are shown where two protons have been detected in coincidence and, in addition, fulfill the momentum conservation condition. The intensity of each pulse was 2×10^{14} W/cm^2. The count rate for nonoverlapping pulses was set to ~ 0.05 ions per laser shot leading to a negligible fraction of false coincidences. For delays close to zero, if the two pulses interfere constructively, the peak intensity is 4 times higher, resulting in a count rate increase of up to 0.5 per shot and, thus, in a noticeable amount of false coincidences in the low-energy region (see [14] for details).

The spectrum of ''true'' coincidences in Fig. 1 can be separated into two parts, with proton energies above and below 2 eV, respectively. Outside the region where the two pulses overlap the high-energy band is delay independent. This structure was observed in numerous previous studies (see, e.g., [4,5,14–18]) and originates from the so-called ''charge-resonance-enhanced ionization'' (CREI) [9] of the H_2^+ molecular ion at internuclear distances R of $\sim$4–7 a.u.. [Atomic units (a.u.) are used throughout the paper if not stated otherwise.] Higher proton energies which can be observed in the region of overlapping pulses are due to the higher laser intensity experienced by the molecule: it was demonstrated that with increasing intensity the CREI peak broadens and shifts to higher energies [15,17].

Here, we concentrate on the region below 2 eV, where a clear delay-dependent structure appears, which is not observed with a single pulse. Starting from the same energy region as the CREI peak, it propagates towards lower and lower energies with increasing delay. Finally, for delays larger than 300 fs, it evolves into two clearly separated bands. This time-dependent structure originates from the process, where the first (pump) pulse ionizes the neutral molecule and induces the dissociation of the molecular ion via Floquet one-photon (1ω) or two-photon (2ω) channels (see the inset of Fig. 1). Depending on the delay of the subsequent probe pulse, which ionizes the dissociating H_2^+ ion at different R, different Coulomb explosion energies of the protons are observed. The measured kinetic energy then consists of the Coulomb energy ($E_C = 1/R$) and the kinetic energy the proton acquired in the dissociation process.

At very large delays the Coulomb repulsion becomes negligible and the energy distribution of the protons from post-dissociative ionization approaches that for the dissociation by a single pulse. Under present conditions, the single-pulse spectrum exhibits two maxima at 0.3 eV for the 1ω and at 0.65 eV for the 2ω channel, respectively. Using these asymptotic values and assuming a classical motion of the protons, we reconstructed the propagation of the dissociating wave packets (dashed lines in Fig. 1). Initial conditions, i.e., $R_{1\omega,2\omega}$ ($\tau = 100$ fs) were chosen in order to fit the experimental data. The good agreement with the experimental data demonstrates that time-resolved CE imaging indeed provides a direct way to map moving nuclear wave packets [6].

The delay-dependent spectrum of the post-dissociative ionization exhibits a noticeable enhancement in the region of 1–1.5 eV kinetic energies (indicated by the arrow in Fig. 1). It might most likely be explained by considering the R dependence of the ionization rate of dissociating H_2^+ molecular ions. Several theoretical studies (see, e.g., [9–12]) have predicted the existence of a second maximum in the ionization probability around $R = 10$ a.u. ($E_C = 1.36$ eV per proton), well beyond the region corresponding to the CREI peak observed in single-pulse measurements (2–4 eV). The enhancement observed in Fig. 1 reflects this second maximum. However, one has to note that in order to extract the R dependence explicitly, it is necessary to clearly disentangle it from the wave packet propagation in the corresponding region of internuclear distances.

In Fig. 2 we present the noncoincident proton kinetic energy spectrum for delays between 17.5 and 45 fs, i.e., for partly overlapping pulses. In contrast to the coincident data of Fig. 1, this spectrum includes both dissociation and CE events. Protons having energies below 1.2 eV originate from the dissociation of H_2^+, whereas fragments with higher kinetic energies are due to the CE channels discussed above. The spectrum exhibits the autocorrelation pattern which considerably changes with increasing delay. Its very left part is quite similar to the case of zero delay,

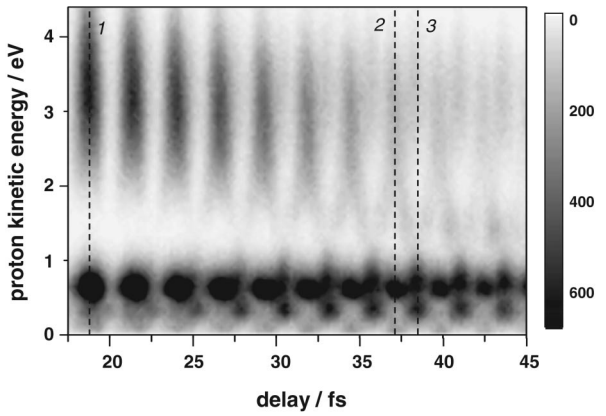

FIG. 2. Noncoincident proton kinetic energy spectrum for the delays from 17.5 to 45 fs. The lines 1, 2, and 3 show the delays corresponding to 7, 14, and 14.5 optical cycles, respectively.

where the constructive interference of two pulses results in a single pulse of the same duration but with 4 times increased intensity, and the destructive one leads to almost complete suppression of the pulse. Accordingly, we observe maxima for all fragmentation channels for the former case (see line 1 in Fig. 2) and almost no counts for the latter. However, for larger delays an increasingly large amount of counts appears as well for destructive interference (line 3), and the corresponding kinetic energy spectrum is clearly different from the constructive situation. In addition, a characteristic delay-dependent ''zigzag'' structure can be observed for proton energies between 1 and 2 eV.

In order to discuss the fragmentation mechanisms in more detail, we display in Fig. 3 the calculated envelopes of the laser intensity profile 3(a) and the proton kinetic energy spectra 3(b) and 3(c) for the cases of constructive and destructive interference between the two pulses, (corresponding to the lines 2 and 3 in Fig. 2, respectively). The coincident spectra [Fig. 3(c)], where only the CE events are included, manifest a clear splitting of the CE peak for destructive interference. Here, as can be seen from Fig. 3(a), the molecule is exposed to a relatively intense laser field for both constructive as well as destructive interference, however, with very different intensity distributions. Whereas constructive interference results in one long pulse with two slight maxima, the destructive case generates two well-separated pulses of lower intensity. Thus, the destructive interference resembles a clean pump-probe scheme, and therefore, we can follow the wave packet dynamics even if two pulses overlap. For the constructive case [open circles in Fig. 3(c)] the second ionization can occur for all time intervals τ_{12} after the removal of the first electron until the pulse falls down, thus, covering the whole range of Coulomb energies from 1 to 4 eV (τ_{12} denotes the time between the first and second ionization step). For the destructive interference, instead, the second step can occur either within the same pulse (first or second), or upon the arrival of the second pulse. This leads to a CE spectrum with two maxima around 3 and 1.5 eV, respectively, (full circles in Fig. 3(c)]. The maximum at 3 eV is formed if both ionization steps occur within the same pulse and is indeed very close to the true single-pulse case (thin line), whereas the peak around 1.5 eV corresponds to the situation where the second pulse ionizes the dissociating H_2^+ ion, created by the first one. For two well-separated pulses [i.e., destructive interference, dashed line in Fig. 3(a)] certain values of τ_{12} cannot contribute, and thus, CE events with energies of about 2 eV, corresponding to these τ_{12}, are missing. The zigzag structure observed in Fig. 2 reflects the molecular response on the changing field configurations, corresponding to all intermediate situations, from two well-separated pulses to one long pulse.

Considering Fig. 3, one can also understand why an additional enhanced ionization maximum, which can be

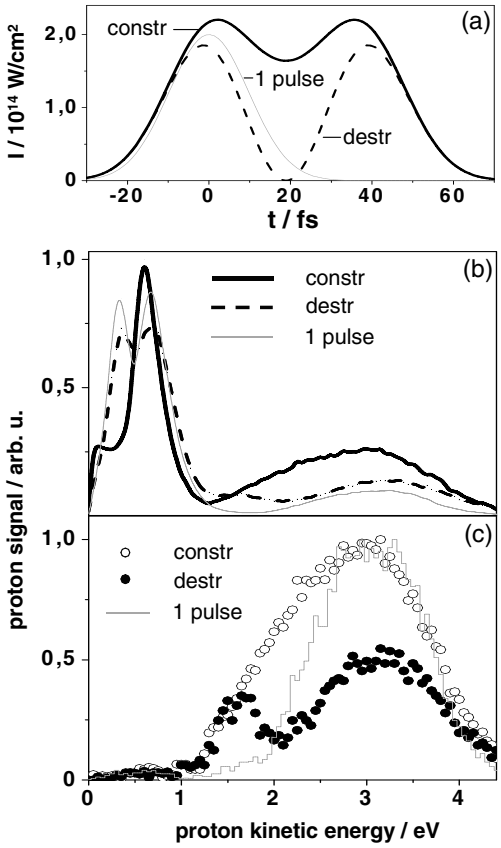

FIG. 3. (a) Time-dependent laser intensity profile for a single pulse (thin gray), and for two pulses separated by the delay of 14 (solid black, line 2 in Fig. 2) and 14.5 (dashed, line 3 in Fig. 2) optical cycles. (b) Corresponding noncoincident proton kinetic energy spectra. The two-pulse data were integrated over the delay region ± 0.3 fs around lines 2 and 3 of Fig. 2 for constructive and destructive case, respectively. Thus, the relative height of these two curves reflects the ionization probabilities for corresponding field configurations, whereas the single-pulse data were arbitrarily normalized for a visual convenience. (c) Same as (b) but measured in coincidence.

observed in Fig. 1, was not resolved in numerous previous experiments on H_2 (D_2). In a single-pulse measurement the laser pulse should be long enough for a molecule to reach the corresponding critical internuclear distances ($\sim$10 a.u.). However, in this case a considerable part of the wave packet will be ionized while passing the first maximum of enhanced ionization ($R \sim 4$–7 a.u.), similar to the constructive case in Fig. 3(c). Thus, the second maximum manifests itself in the spectrum only if one uses two well-separated pulses which are short enough. This situation was partly realized in our recent study on H_2 fragmentation by few-cycle pulses [14] where first indications on the existence of the low-energy CE peak have been obtained. However, due to uncertainties in the pulse shape a definite conclusion could not be drawn.

For the delay region shown in Fig. 2 not only the CE but also the dissociation dynamics differs strongly for the cases of constructive and destructive interferences between the two pulses. For line 3 in Fig. 2 (destructive interference), the low-energy part of the spectrum (up to 1.2 eV) is similar to that obtained with a single pulse [see Fig. 3(b)], indicating that in this case both pulses induce the dissociation independently. For the other case [line 2 in Fig. 2, solid line in Fig. 3(a)] the 1ω dissociation peak is suppressed and shifted towards zero energy, whereas the 2ω peak, being also slightly shifted towards lower energies, is considerably enhanced. This change of the branching ratio is due the differences in the peak intensity and the effective pulse duration [see Fig. 3(a)]. This intensity dependence was already observed experimentally (see, e.g., [18]): the probability of the three-photon transition required for the 2ω channel grows with increasing intensity faster than that of the one-photon process, and, since the H_2^+ ion first passes the three-photon crossing, this results in an enhancement of the 2ω in comparison with the 1ω channel. The effect is further enhanced since for the case of constructive interference the molecule experiences an effectively longer pulse, and it was shown that the 2ω channel has higher relative weight for longer pulse durations [14].

The shift of the 1ω and 2ω peaks towards lower energies is also a consequence of different pulse shapes [16,17]. In [16] it was observed that the 1ω peak shifts to almost zero energy with increasing pulse duration. This effect was attributed to the pulse-length dependent decay dynamics of the so-called ''vibrationally trapped,'' or ''bond hardened'' states. Because of the more efficient trapping for the case of constructive interference we observe a similar shift of the 1ω peak. The origin of the slight shift of the 2ω peak is not yet completely clear. The most likely reason is the difference in the distribution of contributing vibrational states, which depends on both intensity [19] and pulse duration.

In summary, we have shown that time-resolved CE imaging with two 25 fs laser pulses enables a direct mapping of the dissociating nuclear wave packets of H_2^+ molecules. In contrast to earlier pump-probe studies on H_2 [4] and D_2 [5], we were able to separate the motion of the wave packets dissociating via one- and two-photon Floquet channels. In the coincident delay-dependent kinetic energy spectrum we have observed clear signatures of an additional enhanced ionization maximum in the R-dependent ionization probability of H_2^+. Finally, we have demonstrated that our interferometrically stable setup, where the delay between two pulses can be scanned with sub-fs resolution, allows us to extend the pump-probe scheme into the region of partly overlapping pulses, selecting delays for which the pulses interfere destructively. Moreover, we have shown that by changing the electric field profile in a controlled way, one can manipulate the ultrafast molecular fragmentation dynamics, suppressing and enhancing certain fragmentation channels. Vice versa, the possibility of observing an autocorrelation pattern with different fragmentation channels, and thus, with different degree of nonlinearity, opens new ways for *in situ* diagnostics of the laser pulses itself, which is of crucial importance for experiments with few-cycle pulses.

The authors are grateful to M. Lein and A. Saenz for numerous fruitful discussions.

[1] M. G. Raymer, Contemp. Phys. **38**, 343 (1997).
[2] H. Stapelfeldt, E. Constant, and P. B. Corkum, Phys. Rev. Lett. **74**, 3780 (1995).
[3] H. Stapelfeldt, E. Constant, H. Sakai, and P. B. Corkum, Phys. Rev. A **58**, 426 (1998).
[4] J. H. Posthumus *et al.*, J. Phys. B **32**, L93 (1999).
[5] C. Trump, H. Rottke, and W. Sandner, Phys. Rev. A **59**, 2858 (1999).
[6] S. Chelkowski, P. B. Corkum, and A. D. Bandrauk, Phys. Rev. Lett. **82**, 3416 (1999); S. Chelkowski and A. D. Bandrauk, Phys. Rev. A **65**, 023403 (2002).
[7] B. Feuerstein and U. Thumm, Phys. Rev. A **67**, 063408 (2003).
[8] J. H. Posthumus, Rep. Prog. Phys. **67**, 623 (2004).
[9] T. Zuo and A. D. Bandrauk, Phys. Rev. A **52**, R2511 (1995).
[10] M. Plummer and J. F. McCann, J. Phys. B **29**, 4625 (1996).
[11] L.-Y. Peng, D. Dundas, J. F. McCann, K. T. Taylor, and I. D. Williams, J. Phys. B **36**, L295 (2003).
[12] M. Vafaee and H. Sabzyan, J. Phys. B **37**, 4143 (2004).
[13] V. L. B. de Jesus *et al.*, J. Electron Spectrosc. Relat. Phenom. **141**, 127 (2004).
[14] A. Rudenko *et al.*, J. Phys. B **38**, 487 (2005).
[15] T. D. G. Walsh, F. A. Ilkow, and S. I. Chin, J. Phys. B **30**, 2167 (1997).
[16] L. J. Frasinski *et al.*, Phys. Rev. Lett. **83**, 3625 (1999).
[17] C. Trump *et al.*, Phys. Rev. A **62**, 063402 (2000).
[18] A. Staudte *et al.*, Phys. Rev. A **65**, 020703(R) (2002).
[19] X. Urbain *et al.*, Phys. Rev. Lett. **92**, 163004 (2004).
[20] P. H. Bucksbaum, A. Zavriyev, H. G. Muller, and D. W. Schumacher, Phys. Rev. Lett. **64**, 1883 (1990).